



Dye Removal from Single and Quaternary Systems Using Surface Modified Nanoparticles: Isotherm and Kinetics Studies

N. M. Mahmoodi* and S. Soltani-Gordefaramarzi

Department of Environmental Research, Institute for Color Science and Technology, P. O. Box: 16765-654, Tehran, Iran.

ARTICLE INFO

Article history:

Received: 25 Jan 2016

Final Revised: 08 Mar 2016

Accepted: 10 Apr 2016

Available online: 10 Apr 2016

Keywords:

Quaternary system

Dye removal

Surface modified nanoparticle

Isotherm

Kinetic

ABSTRACT

In this paper, dye removal ability of the surface modified nanoparticle (SMN) (copper ferrite) using surfactant (cetyl trimethyl ammonium bromide (CTAB)) from single and quaternary systems was investigated. Acid Blue 92 (AB92), Direct Green 6 (DG6), Direct Red 23 (DR23) and Direct Red 80 (DR80) were used as model compounds. The effect of surfactant concentration, adsorbent dosage, dye concentration and pH on dye removal was evaluated. The adsorption isotherm and kinetic were also studied. The maximum dye adsorption capacity (Q_0) was 178.571 mg/g AB92, 49.261 mg/g DG6, 39.841 mg/g DR23 and 43.290 mg/g DR80 for SMN. It was found that dye adsorption onto SMN followed Langmuir isotherm. Adsorption kinetic of dyes was found to conform to pseudo-second order kinetics. Prog. Color Colorants Coat. 9 (2016), 85-97 © Institute for Color Science and Technology.

1. Introduction

Treatment of colored wastewaters is one of the main concerns of environmental scientists and engineers because some dyes produce toxic and carcinogenic byproducts via hydrolysis, oxidation, etc. [1-10]. Dye removal using adsorbents is one of the wastewater treatment methods. Natural polymers such as chitosan are used to remove dyes. Chitosan is the N-deacetylated derivative of chitin [11, 12]. Some adsorbents have low dye adsorption capacity and poor separation ability. Thus, researchers interest to conquer these adsorbent limitations.

The magnetic nanoparticles as adsorbents could be separated based on their nanostructures since the ease of direction of magnetization would vary depending on

the ordering of atoms in the magnetic structure [13-19]. The main limitation of some magnetic adsorbents is their low pollutant removal potential. To conquest this disadvantage, the surface of magnetic nanoparticles was modified using surfactants. The surface properties of nanoparticles can be greatly modified with a surfactant. This is favored by van der Waals interaction between surfactant and the reduced solvent shielding of the ions in the interlamellar environment. In addition, surfactant provides corrosion inhibition effect [20].

A literature review showed that surface modified nanoparticle (SMN) (copper ferrite) using cetyltrimethylammonium bromide (CTAB) was not used to remove dyes from Quaternary systems.

*Corresponding author: mahmoodi@icrc.ac.ir

In this paper, dye removal ability of surface modified copper ferrite nanoparticle (SMN) from single and quaternary systems is investigated. Acid Blue 92 (AB92), Direct Green 6 (DG6), Direct Red 23 (DR23) and Direct Red 80 (DR80) are used as model compounds. The effect of operational parameters (i.e. surfactant concentration, adsorbent dosage, dye concentration and pH) on dye removal is evaluated. The isotherm and kinetics of dye adsorption are also studied.

2. Experimental

2.1. Materials

Acid Blue 92 (AB92), Direct Green 6 (DG6), Direct Red 23 (DR23) and Direct Red 80 (DR80) were

obtained from Ciba and used without further purification. The chemical structure of dyes is shown in Figure 1. Other chemicals were of analytical grade and obtained from Merck.

2.2. Synthesis of copper ferrite and SMN

2.2.1 Synthesis of copper ferrite

4.90 g copper nitrate and 13.4 g iron nitrate was dissolved in 50 mL distilled water which was then added to an aqueous mixed solution of 4.2 g NaOH in 70 mL distilled water and 3 mL ethylene diamine (EG). This solution was heated at 90 °C for 1 h to achieve complete chelation. The powder was calcined on alumina crucible at 500 °C for 1 h, with a heating rate of 10 °C/min [21].

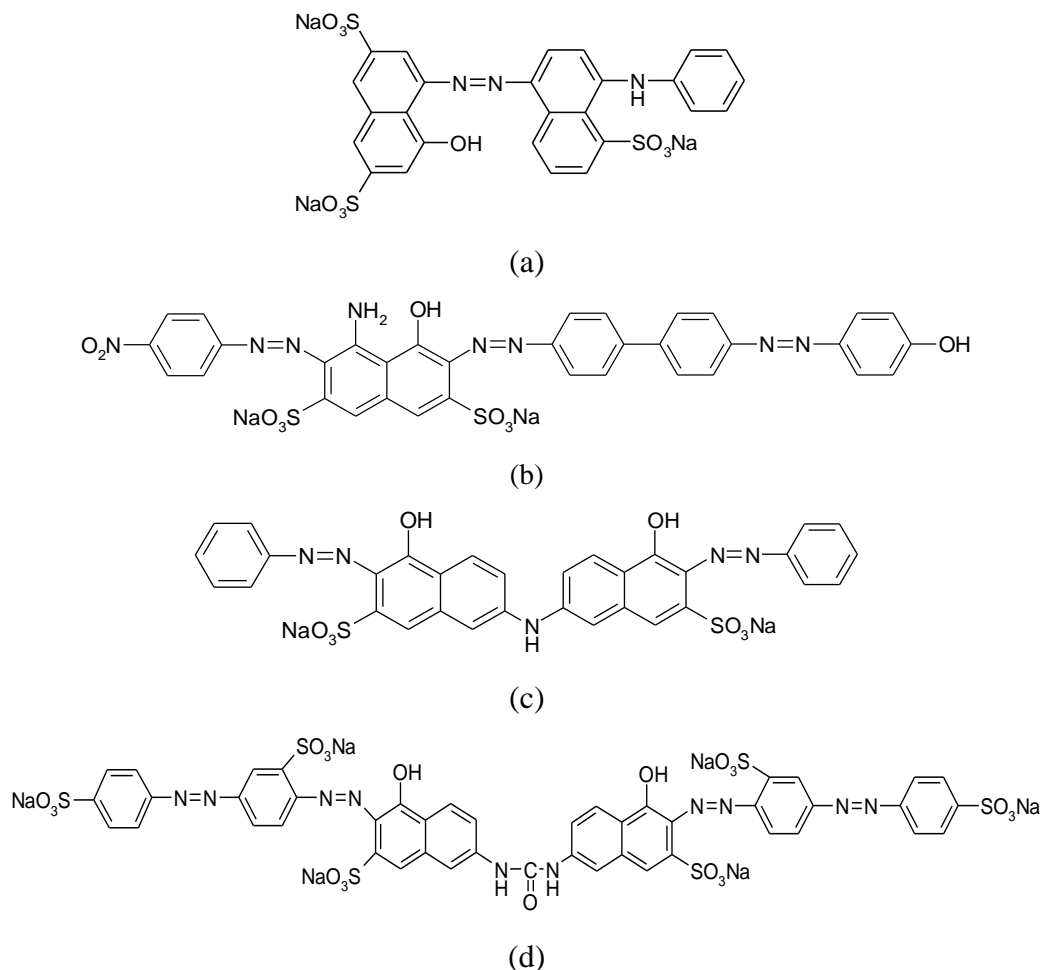


Figure 1: The chemical structure of dyes: (a) AB92, (b) DG6, (c) DR23 and (d) DR80.

2.2.2 Synthesis of SMN

CTAB (0.4 g) was added to a solution containing 10 mL acetone, 125 mL distilled water and 1 g copper ferrite. The mixture was stirred in a mixer for 1 h. The organo-modified copper ferrite was separated from the mixture by magnetic force and then was washed with distilled water [21].

2.3. Adsorption procedure

The dye adsorption measurements were conducted by mixing of adsorbent in jars containing 250 mL dye solution (50 mg/L). The solution pH was adjusted by adding H₂SO₄ or NaOH. The absorbance of all samples were monitored and determined at certain time intervals during the adsorption process. At the end of the adsorption experiments, the adsorbent particles were removed from the solution by magnetic separation using a magnet and the dye concentration was determined. The results were verified with the adsorption kinetics and isotherms.

UV-Vis Perkin-Elmer Lambda 25 spectrophotometer was employed for absorbance measurements of samples. The maximum wavelengths (λ_{max}) used for determination of residual concentration of AB25, DG6, DR23 and DR80 in supernatant solution using UV-VIS spectrophotometer were 580 nm, 632 nm, 500 nm and 540 nm, respectively. The solution pH was adjusted by adding H₂SO₄ or NaOH.

The isotherm and kinetics of dye adsorption on SMN were studied by contacting 250 mL of dye solution with initial dye concentration of 50 mg/L for 60 min at different amounts of SMN.

The effect of surfactant concentration on dye removal was investigated by contacting 250 mL of dye solution with initial dye concentration of 50 mg/L for 60 min. The effect of adsorbent dosage on dye removal was investigated by contacting 250 mL of dye solution with initial dye concentration of 50 mg/L for 60 min. The effect of initial dye concentration (50-200 mg/L) on dye removal was investigated by contacting 250 mL of dye solution with SMN for 60 min. The effect of pH on dye removal was investigated by contacting 250 mL of dye solution with initial dye concentration (50 mg/L) for 60 min.

3. Results and discussion

3.1. Effect of operation parameters on dye

removal

3.1.1. Effect of surfactant concentration

The dye removal (%) versus time (min) at different surfactant concentrations is shown in Figure 2. The increase in dye adsorption with surfactant concentration is due to higher availability of adsorption sites. An electrostatic attraction exists between the positively charged (-N⁺) surface of the SMN by surfactant and negatively charged anionic dyes.

3.1.2. Effect of adsorbent dosage

The dye removal (%) versus time (min) at different SMN dosages (g) is shown in Figure 3. The increase in dye adsorption with adsorbent dosage is due to the increasing of adsorbent surface and availability of more adsorption sites. However, if the adsorption capacity was expressed in mg adsorbed per gram of material, the capacity decreases by increasing the amount of adsorbent. It can be attributed to overlapping or aggregation of adsorption sites resulting in a decrease in total adsorbent surface area available to the dye and an increase in diffusion path length [22].

3.1.3. Effect of dye concentration

Adsorption can generally be defined as the accumulation of material at the interface between two phases [22]. The influence of initial dye concentration on adsorption efficiencies onto SMN was assessed. The results are shown in Figure 4. It is obvious that the higher the initial dye concentration, the lower the percentage of dye adsorbed. The amount of the dye adsorbed onto SMN increases with the initial dye concentration in solution if the amount of adsorbent is kept unchanged due to the increase in the driving force of the concentration gradient with the higher initial dye concentration. The adsorption of dye by SMN is very intense and reaches equilibrium very quickly at low initial concentrations. At a fixed SMN dosage, the amount of adsorbed dye increased with increasing the solution concentration, but the percentage of adsorption decreased. In other words, the concentration of residual dye will be higher for higher initial dye concentrations. In the case of lower concentrations, the ratio of initial number of dye moles to the available adsorption sites is low and subsequently the fractional adsorption becomes independent of initial concentration [22].

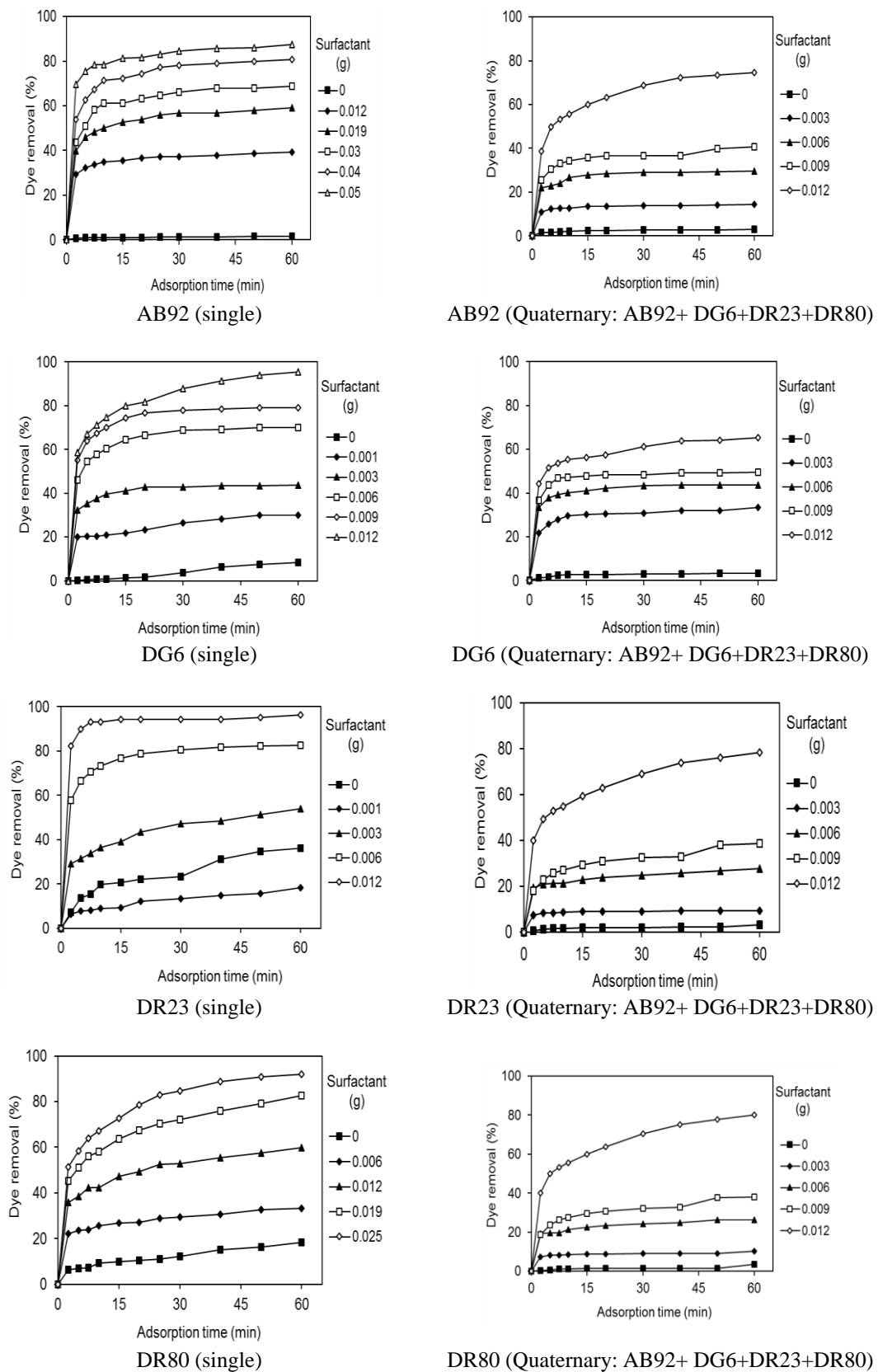


Figure 2: The effect of surfactant concentration on the modification of nanoparticles to remove dyes from single and quaternary systems.

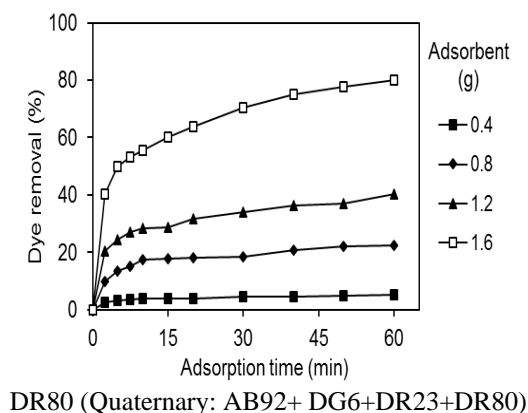
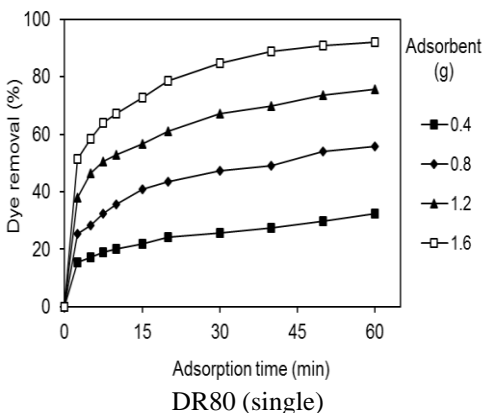
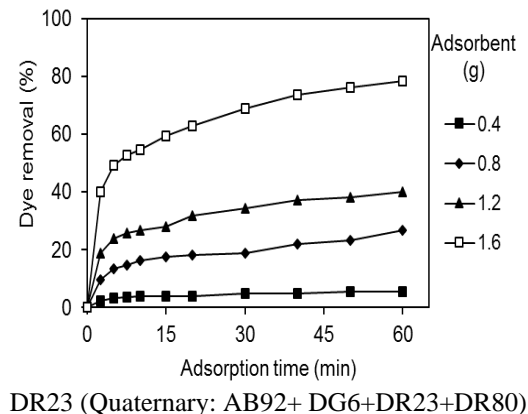
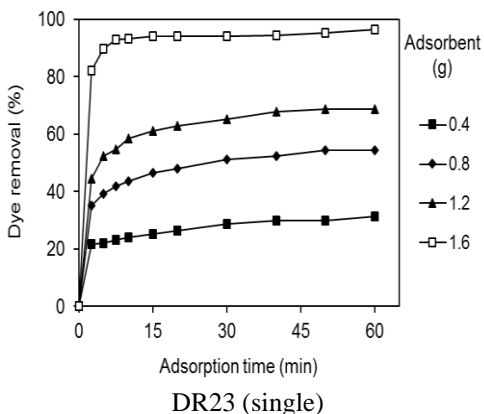
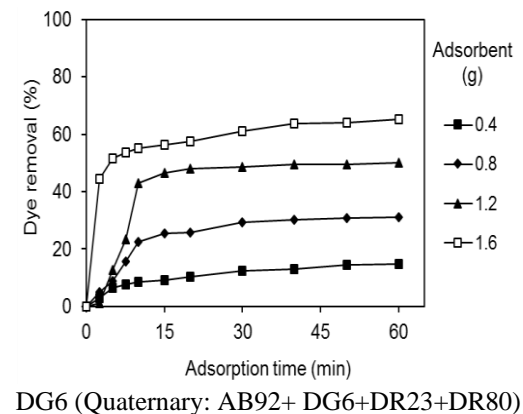
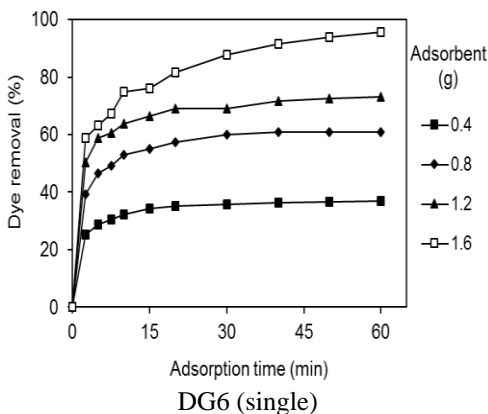
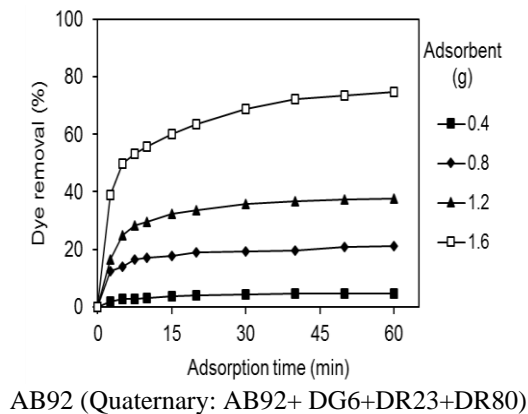
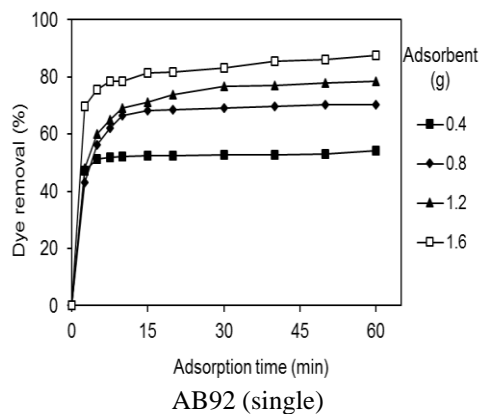


Figure 3: The effect of SMN dosage on dye removal using SMN from single and quaternary systems.

3.1.4. The effect of pH

The effect of pH on the adsorption of dyes onto SMN is shown in Figure 5. At various pH values, the electrostatic attraction as well as the organic property and chemical structure of dye molecules and SMN

could play very important roles in dye adsorption on SMN. The adsorption capacity does not change when the pH changes. It can be attributed that positively charged group of surfactant does not change with the solution pH.

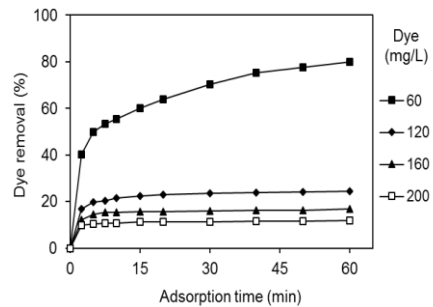
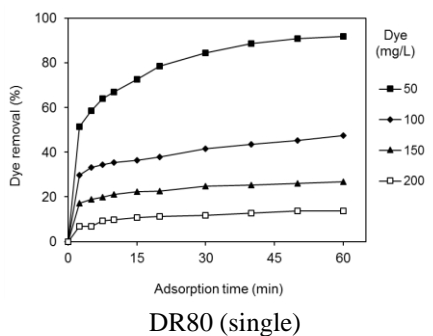
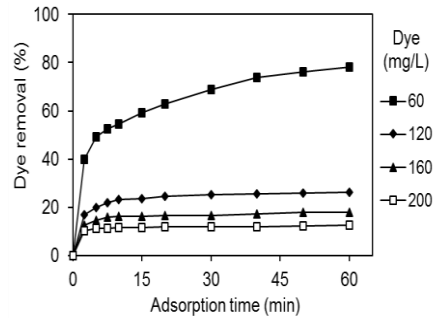
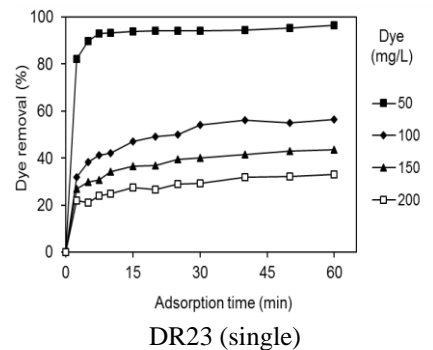
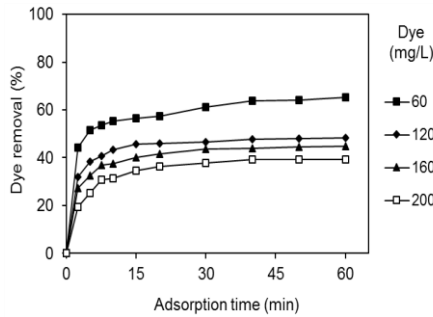
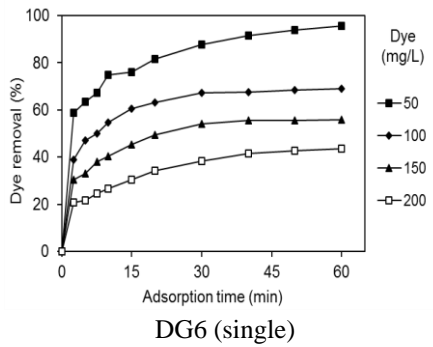
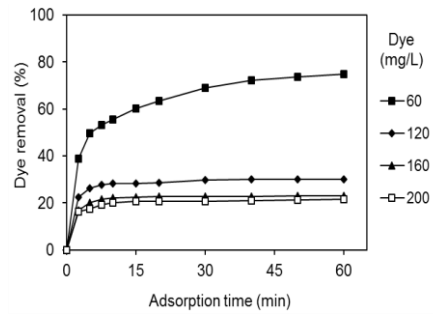
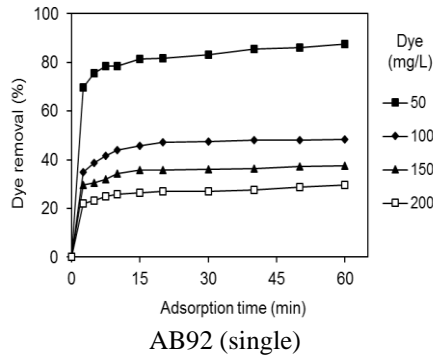


Figure 4: The effect of dye concentration on dye removal using SMN from single and quaternary systems.

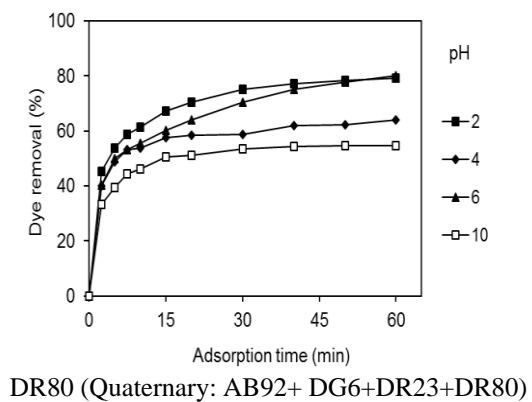
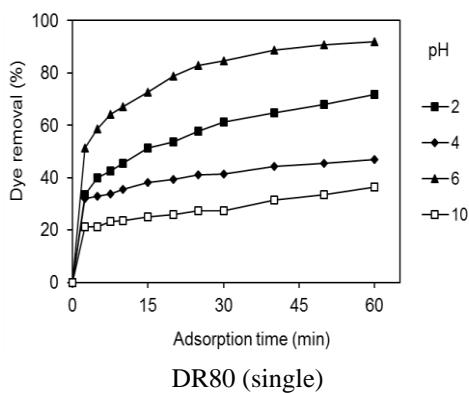
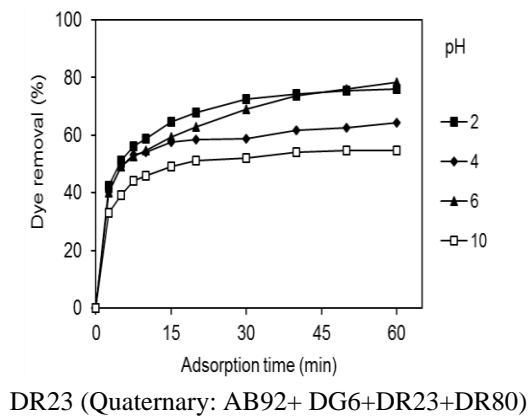
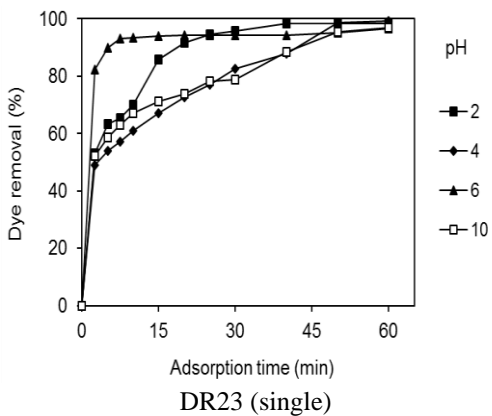
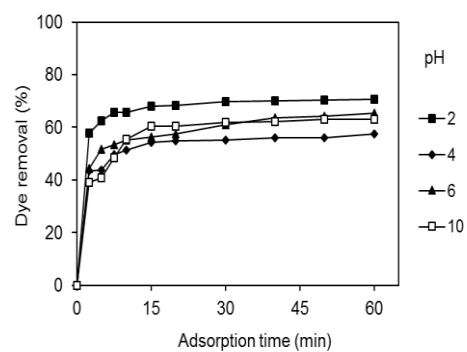
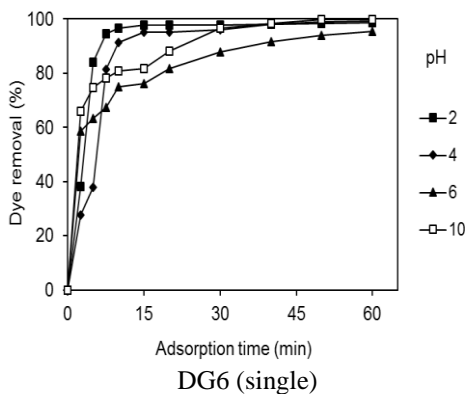
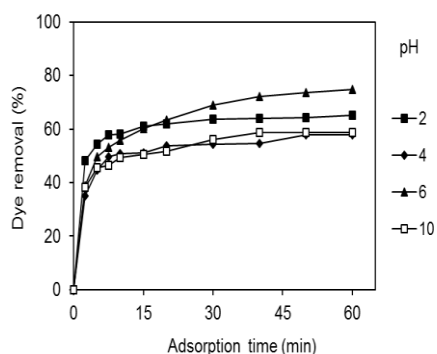
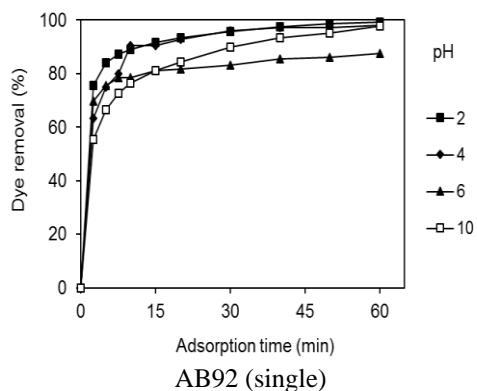


Figure 5: The effect of pH on dye removal using SMN from single and quaternary systems.

3.3. Adsorption isotherms

The relation between the mass of the dye adsorbed at a particular temperature, pH, particle size and liquid phase of the dye concentration is evaluated using adsorption isotherms [23-25]. The current research presents a method of direct comparison of the isotherm fit of several models (the Langmuir, Freundlich and Tempkin models) to enable the best-fit and the best isotherm parameters to be obtained.

The Langmuir isotherm explains the adsorption of dye into adsorbent. A basic assumption of the Langmuir theory is that adsorption takes place at specific sites within the adsorbent [26]. The Langmuir equation can be written as follows:

$$q_e = Q_0 K_L C_e / (1 + K_L C_e) \tag{1}$$

where q_e , C_e , K_L and Q_0 are the amount of dye adsorbed at equilibrium (mg/g), the equilibrium concentration of dye solution (mg/L), Langmuir constant (L/g) and the maximum adsorption capacity (mg/g), respectively. The linear form of Langmuir equation is:

$$C_e/q_e = 1/K_L Q_0 + C_e/Q_0 \tag{2}$$

The Freundlich model can also be used for evaluating isotherm data [27]:

$$q_e = K_F C_e^{1/n} \tag{3}$$

where K_F is adsorption capacity at unit concentration and $1/n$ is adsorption intensity. Eq. (3)

can be rearranged to a linear form:

$$\log q_e = \log K_F + (1/n) \log C_e \tag{4}$$

The Tempkin isotherm is given as [28]:

$$q_e = B_1 \ln K_T + B_1 \ln C_e \tag{5}$$

where

$$B_1 = RT/b \tag{6}$$

A plot of q_e versus $\ln C_e$ enables the determination of the isotherm constants B_1 and K_T from the slope and the intercept, respectively. K_T is the equilibrium binding constant (L/mg) corresponding to the maximum binding energy and constant B_1 is related to the heat of adsorption.

To study the applicability of the Langmuir, Freundlich and Tempkin isotherms for the dye adsorption onto SMN at different adsorbent dosages, linear plots of C_e/q_e against C_e , $\log q_e$ versus $\log C_e$ and q_e versus $\ln C_e$ are plotted. The values of Q_0 , K_L , K_F , $1/n$, K_T , B_1 and R^2 are listed in Table 1.

The R^2 values show that the dye removal isotherm using SMN does not follow the Freundlich and Tempkin isotherms (Table 1). The linear fit between the C_e/q_e versus C_e and the calculated R^2 values for Langmuir isotherm model shows that the dye removal isotherm can be approximated as Langmuir model (Table 1). This means that the adsorption of dyes takes place at specific homogeneous sites and a one layer adsorption onto SMN surface.

Table 1: Linearized isotherm coefficients for dye adsorption onto SMN at different adsorbent dosages.

Dye	Langmuir			Freundlich			Tempkin		
	Q_0	K_L	R^2	K_F	$1/n$	R^2	K_T	B_1	R^2
AB92	178.571	0.024	0.573	6.923	0.703	0.942	0.329	30.710	0.882
DG6	49.261	0.227	0.935	25.235	0.140	0.615	101.932	5.103	0.596
DR23	39.841	0.353	0.963	27.932	0.064	0.374	334430.560	2.168	0.382
DR80	43.290	0.285	0.984	22.491	0.154	0.895	0.020	5.198	0.863

4.3. Adsorption kinetics

Adsorption kinetic was determined using pseudo-first order equation, pseudo-second order equation and intraparticle diffusion model [29] in order to investigate the mechanism of dye adsorption onto SMN.

A linear form of pseudo-first order model is [29]:

$$\log (q_e - q_t) = \log (q_e) - (k_1/2.303) t \quad (7)$$

where q_t and k_1 are the amount of dye adsorbed at time t (mg/g) and the equilibrium rate constant of pseudo-first order kinetics ($1/min$), respectively.

Linear form of pseudo-second order model is defined as [29]:

$$t/q_t = 1/k_2 q_e^2 + (1/q_e)t \quad (8)$$

where k_2 is the equilibrium rate constant of pseudo-second order (g/mg min).

The possibility of intraparticle diffusion resistance affecting adsorption was explored by using the intraparticle diffusion model as [29]:

$$q_t = k_p t^{1/2} + I \quad (9)$$

where k_p and I are the intraparticle diffusion rate constant and intercept, respectively.

To understand the applicability of the pseudo first-order, pseudo second-order and intraparticle diffusion models for the dye adsorption onto SMN at different adsorbent dosages, linear plots of $\log(q_e - q_t)$ versus contact time (t) (Figure 6), t/q_t versus contact time (t) (Figure 7) and q_t against $t^{1/2}$ (Figure 8) are plotted. The values of k_1 , k_2 , k_p , I , R^2 (correlation coefficient values) and the calculated q_e ($(q_e)_{Cal.}$) are shown in Table 2. R^2 demonstrates that pseudo-first order and intraparticle diffusion kinetic models do not play a significant role in the uptake of the dye by SMN (Table 2). The linear fit between the t/q_t versus contact time (t) and the calculated R^2 values for pseudo-second order kinetics model show that the dye removal kinetic can be approximated as pseudo-second order kinetics (Table 2). In addition, the experimental q_e ($(q_e)_{Exp.}$) values agree with the calculated ones ($(q_e)_{Cal.}$) obtained from the linear plots of pseudo-second order kinetics (Table 2).

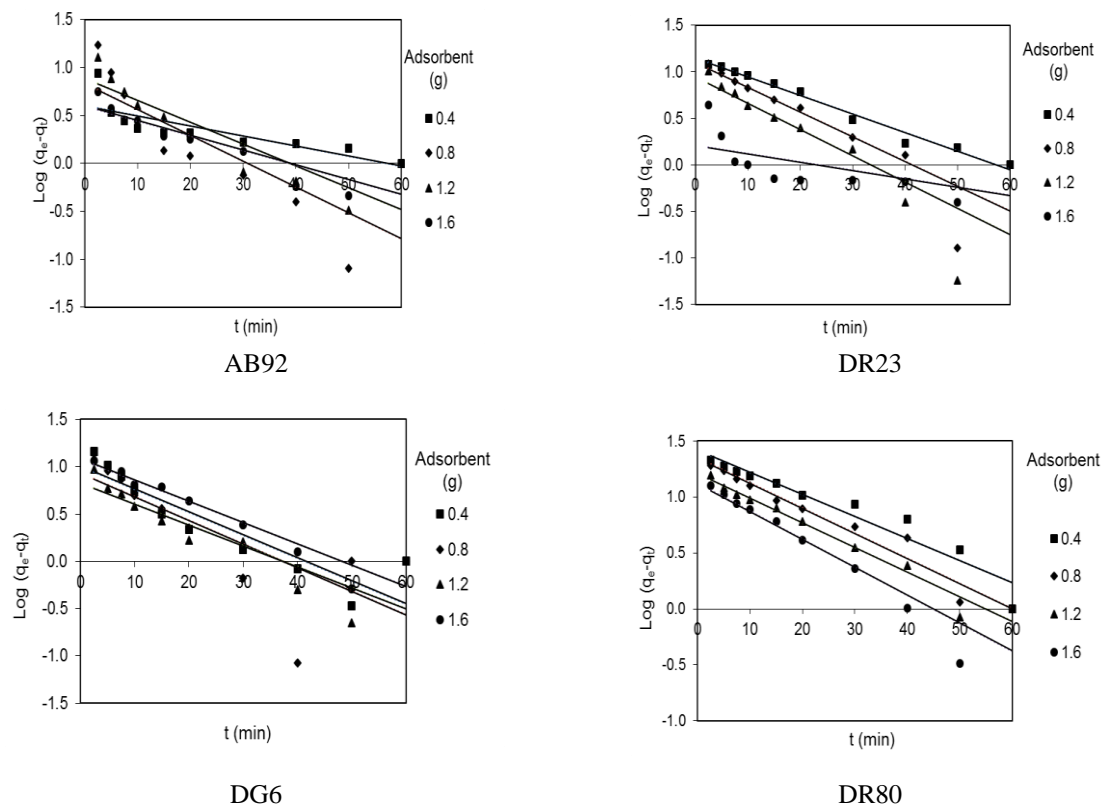


Figure 6: Pseudo-first order kinetics of dye removal by SMN.

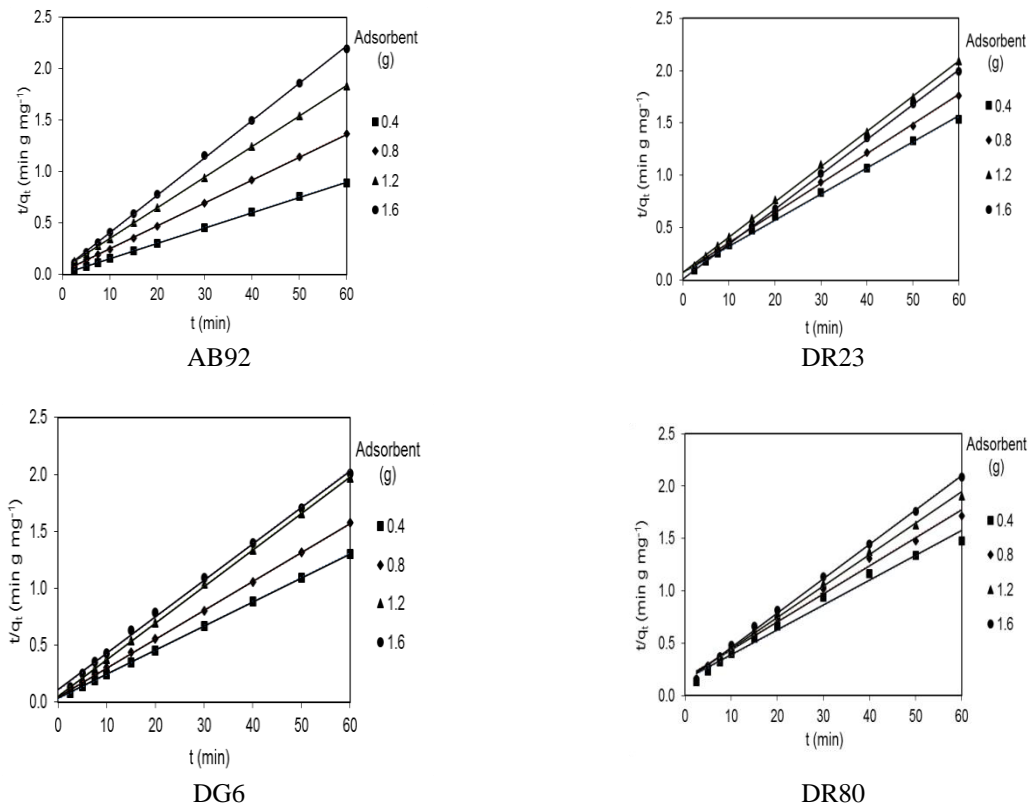


Figure 7: Pseudo-second order kinetics of dye removal by SMN.

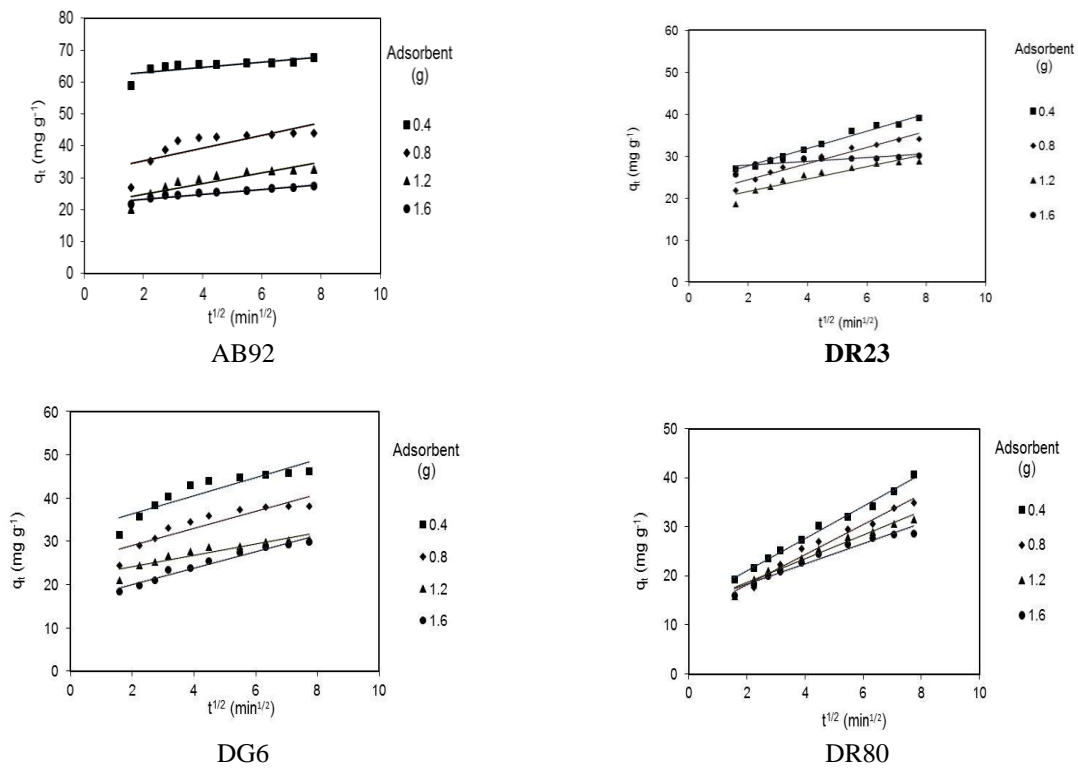


Figure 8: Intraparticle diffusion kinetics of dye removal by SMN.

Table 2: Linearized kinetic coefficients for dye adsorption onto SMN at different adsorbent dosages.

Dye	Adsorbent (g)	$(q_e)_{Exp}$	Pseudo-first order			Pseudo-second order			Intraparticle diffusion		
			$(q_e)_{Cal.}$	k_1	R^2	$(q_e)_{Cal.}$	k_2	R^2	k_p	I	R^2
AB92	0.400	67.602	3.994	0.024	0.679	67.114	0.037	0.999	0.828	61.294	0.572
	0.800	43.965	6.827	0.062	0.646	44.843	0.019	0.999	1.988	31.355	0.595
	1.200	32.744	7.665	0.053	0.788	33.670	0.017	1.000	1.678	21.557	0.776
	1.600	27.324	3.971	0.035	0.790	27.548	0.032	0.999	0.756	21.846	0.892
DG6	0.400	46.141	0.946	0.056	0.832	47.170	0.014	0.999	2.096	32.130	0.814
	0.800	38.087	8.541	0.058	0.576	39.370	0.014	0.999	1.983	25.068	0.829
	1.200	30.425	6.685	0.051	0.772	31.056	0.020	0.999	1.305	21.495	0.845
	1.600	29.860	12.109	0.052	0.927	31.153	0.009	0.998	1.906	16.190	0.964
DR23	0.400	39.046	0.955	0.046	0.984	40.161	0.008	0.997	2.070	23.543	0.984
	0.800	34.048	12.540	0.061	0.787	35.336	0.011	0.999	1.917	20.591	0.947
	1.200	28.680	8.831	0.065	0.702	29.674	0.016	0.999	1.487	18.546	0.887
	1.600	30.143	1.617	0.021	0.374	30.120	0.080	0.999	0.447	26.978	0.561
DR80	0.400	40.657	26.026	0.045	0.927	42.194	0.001	0.985	3.279	14.524	0.992
	0.800	34.957	22.187	0.052	0.964	37.313	0.001	0.993	3.088	11.980	0.976
	1.200	31.489	16.207	0.051	0.972	33.223	0.001	0.996	2.411	13.865	0.971
	1.600	28.719	13.195	0.057	0.886	30.395	0.001	0.998	2.073	14.120	0.960

4.4. Dye removal mechanism by SMN

Copper ferrite has negative charge on its surface and thus not suitable for adsorption of anionic dyes. Thus, its surface should be modified. The surface modification of copper ferrite by adsorption of cationic surfactant has four steps. In step I, when the surfactant concentration is low (much lower than the critical micelle concentration (CMC) of the surfactant), surfactant moieties are adsorbed to the negatively charged substrate almost exclusively by ion exchange mechanism. Thus, the counter ions in the diffuse double layer just outside the surface are exchanged for surfactants with the same charge. This ion exchange leads to a higher surfactant concentration at the surface than that in the bulk. Step II involves a strong lateral interaction between adsorbed monomers as a result of hydrophobic interactions between alkyl tails of the surfactants, resulting in the formation of primary aggregates. The previous published papers have shown that the surfactants are adsorbed with head-groups facing towards the surface while the hydrocarbon tail-groups protrude into solution [30-33]. This creates

hydrophobic patches on the surface. By increasing the concentration of surfactant in the solution, the packing at the surface increases as can be seen in step III. At concentrations above CMC, the surfactants form a double layer (step IV) [30]. The modification of copper ferrite with CTAB (SMN) provides many cationic sites at the surface of the particles which can be used for adsorption of anionic dyes by electrostatic attraction.

4. Conclusion

Dye removal ability of SMN from single and quaternary systems was investigated. Acid Blue 92 (AB92), Direct Green 6 (DG6), Direct Red 23 (DR23) and Direct Red 80 (DR80) were used as model compounds. It was found that dye adsorption onto SMN followed the Langmuir isotherm. Adsorption kinetics of dyes was found to conform to pseudo-second order kinetics. It can be concluded that the SMN as a magnetic material might be a suitable alternative to remove dyes from colored aqueous solutions.

6. References

- G. Vijayaraghavan, S. Shanthakumar. Performance study on algal alginate as natural coagulant for the removal of Congo red dye. *Desalin. Water Treat.* 57(2016), 6384-6392.
- K. Khelif, Z. Salem, L. Boumehti. Dye removal by incineration residues of pharmaceutical wastes in aqueous solution. *Desalin. Water Treat.* 57(2016), 6063-6071.
- A. R. Tehrani-Bagha, F. L. Amini. Decolorization of a Reactive Dye by UV-Enhanced Ozonation. *Prog. Color Colorants Coat.* 3(2010), 1-8.
- M. R. Patil, V. S. Shrivastava. Adsorptive removal of methylene blue from aqueous solution by polyaniline-nickel ferrite nanocomposite: a kinetic approach. *Desalin. Water Treat.* 57(2016), 5879-5887.
- D. Marmanis, K. Dermentzis, A. Christoforidis, K. Ouzounis, A. Moutzakis. Electrochemical treatment of actual dye house effluents using electrocoagulation process directly powered by photovoltaic energy. *Desalin. Water Treat.* 56(2015), 2988-2993.
- T. Poursaberi. Magnetic Removal of Acid Dyes from Wastewater with Ionic Liquid Linked-Nanoparticles. *Prog. Color Colorants Coat.* 7(2014), 27-38.
- A. Verma, A. K. Hura, D. Dixit. Sequential photo-Fenton and sono-photo-Fenton degradation studies of Reactive Black 5 (RB5). *Desalin. Water Treat.* 56(2015), 677-683.
- N. M. Mahmoodi. Synthesis of amine-functionalized magnetic ferrite nanoparticle and its dye removal ability. *J. Environ. Eng.* 139(2013), 1382-1390.
- N. M. Mahmoodi, Zinc ferrite nanoparticle as a magnetic catalyst: synthesis and dye degradation. *Mater. Res. Bull.* 48(2013), 4255-4260.
- N. M. Mahmoodi. Photocatalytic ozonation of dyes using multiwalled carbon nanotube. *J. Mole. Catal. A: Chem.* 366(2013), 254-260.
- S. Davarpanah, N. M. Mahmoodi, M. Arami, H. Bahrami, F. Mazaheri. Environmentally friendly surface modification of silk fiber: chitosan grafting and dyeing. *Appl. Surf. Sci.* 255(2009), 4171-4176.
- M. Ranjbar-Mohammadi, M. Arami, H. Bahrami, F. Mazaheri, N. M. Mahmoodi. Grafting of chitosan as a biopolymer onto wool fabric using anhydride bridge and its antibacterial property. *Colloid. Surface. B.* 76(2010), 397-403.
- R. D. Ambashta, M. Sillanpää, Water purification using magnetic assistance: A review, *J. Hazard. Mater.* 180(2010), 38-49.
- J. L. Gong, B. Wang, G. M. Zeng, C. P. Yang, C.G. Niu, Q.Y. Niu, W.J. Zhou, Y. Liang, Removal of cationic dyes from aqueous solution using magnetic multi-wall carbon nanotube nanocomposite as adsorbent. *J. Hazard. Mater.* 164(2009), 1517-1522.
- S. Qadri, A. Ganoie, Y. Haik, Removal and recovery of acridine orange from solutions by use of magnetic Nanoparticles. *J. Hazard. Mater.* 169(2009), 318-323.
- S. Qu, F. Huang, S. Yu, G. Chen, J. Kong, Magnetic removal of dyes from aqueous solution using multi-walled carbon nanotubes filled with Fe₂O₃ particles, *J. Hazard. Mater.* 160(2008), 643-647.
- V. Rocher, J. M. Siaugue, V. Cabuil, A. Bee, Removal of organic dyes by magnetic alginate beads, *Water Res.* 42(2008), 1290-1298.
- J. Sun, R. Xu, Y. Zhang, M. Ma, N. Gu, Magnetic nanoparticles separation based on nanostructures, *J. Magn. Magn. Mater.* 312(2007), 354-358.
- A. F. Ngomsik, A. Bee, M. Draye, G. Cote, V. Cabuil, Magnetic nano- and microparticles for metal removal and environmental applications: a review. *C. R. Chimie.* 8(2005), 963-970.
- D. Asefi, N. M. Mahmoodi, M. Arami, Effect of nonionic co-surfactants on corrosion inhibition effect of cationic gemini surfactant. *Colloid. Surface. A.* 355(2010), 183-186.
- N. M. Mahmoodi, S. Soltani-Gordefaramarzi, M. Sadeghi-Kiakhani. Dye removal using modified copper ferrite nanoparticle and RSM analysis. *Environ. Monit. Assess.* 185(2013), 10235-10248.
- G. Crini, P. M. Badot, Application of chitosan, a natural aminopolysaccharide, for dye removal from aqueous solutions by adsorption processes using batch studies: A review of recent literature. *Prog. Polym. Sci.* 33(2008), 399-447.
- M. Uğurlu, Adsorption of a textile dye onto activated sepiolite. *Micropor. Mesopor. Mater.* 119(2009), 276-283.
- Y. Bulut, H. Aydin, A kinetics and thermodynamics study of methylene blue adsorption on wheat shells. *Desalination.* 194(2006), 259-267.
- N. K. Amin, Removal of reactive dye from aqueous solutions by adsorption onto activated carbons prepared from sugarcane bagasse pith. *Desalination.* 223(2008), 152-161.
- F. Chen, L. Xiong, M. Cai, W. Xu, X. Liu. Adsorption of direct fast scarlet 4BS dye from aqueous solution onto natural superfine down particle. *Fibers Polym.* 16(2015), 73-78.

27. C. Hou, H. Yang, Z. L. Xu, Y. M. Wei. Preparation of PAN/PAMAM blend nanofiber mats as efficient adsorbent for dye removal. *Fibers Polym.* 16(2015), 1917-1924.
28. M. J. Tempkin, V. Pyzhev, Recent modification to Langmuir isotherms. *Acta Physiochim. USSR.* 12(1940), 217-222.
29. A. Altinisik, Y. Seki, S. Ertas, E. Akar, E. Bozacı, Y. Seki. Evaluating of Agave Americana fibers for biosorption of dye from aqueous solution. *Fibers Polym.* 16(2015) 370-377.
30. R. Atkin, V. S. J. Craig E. J. Wanless, S. Biggs. Mechanism of cationic surfactant adsorption at the solid–aqueous interface. *Adv. Colloid Interfac. Sci.* 103(2003), 219-304.
31. A. Fan, P. Somasundaran, N. J. Turro. Adsorption of Alkyltrimethyl-ammonium Bromides on Negatively Charged Alumina. *Langmuir.* 13(1997), 506-510.
32. P. Somasundaran, C. V. Kunjappu, C. V. Kumar, N. J. Turro, J. K. Barton, Excited State Resonance Raman Spectroscopy as a Probe of Alumina-Sodium Dodecyl Sulfate Hemimicelles. *Langmuir.* 5(1989), 215-218.
33. N. M. Mahmoodi, M. Banijamali, B. Noroozi. Surface modification and ternary system dye removal ability of manganese ferrite nanoparticle. *Fibers Polym.* 15(2014), 1616-1626.

How to cite this article:

N. M. Mahmoodi, S. Soltani-Gordefaramarzi, Dye Removal from Single and Quaternary Systems Using Surface Modified Nanoparticles: Isotherm and Kinetics Studies, *Prog. Color Colorants Coat.*, 9 (2016) 85-97.

